PPPL-3227, Preprint: January 1997, UC-426

MEASUREMENT OF THE HOT ELECTRICAL CONDUCTIVITY IN THE PBX-M TOKAMAK

G. Giruzzi[a] , E. Barbato[b], S. Bernabei[c], A. Cardinali[b]

[a]*Association EURATOM-CEA sur la Fusion, Département de Recherches sur la Fusion Contrôlée, CEA/Cadarache, 13108 St. Paul-lez-Durance (FRANCE)*

[b]*Associazione EURATOM-ENEA sulla Fusione, Centro Ricerche Energia Frascati, C.P. 65, 00044 Frascati (ITALY)*

[c]*Plasma Physics Laboratory, Princeton University, Princeton, NJ 08543 (USA)*

Abstract

A new method for the analysis of tokamak discharges in which the plasma current is driven by the combination of high-power rf waves and a dc electric field is presented. In such regimes, which are the most usual in rf current drive experiments, it is generally difficult to separate the different components of the plasma current, i.e., purely Ohmic, purely non-inductive and cross terms. If the bilinear (in wave power and electric field) cross term is the dominant one, an explicit relation between the loop voltage drop and the injected power can be found. This relation involves two parameters, the purely rf current drive efficiency and the hot (power dependent) electrical conductivity. These can be simultaneously determined from a simple two-parameter fit, if the loop voltage drop is measured at several rf power levels. An application to lower hybrid current drive experiments in the PBX-M tokamak is presented. It is shown that the method also allows the independent evaluation of the average power absorption fraction and $n_{||}$ upshift.

1. Introduction

Radiofrequency waves have proved the capability of driving the current necessary for the stability of tokamak plasmas, without any contribution from the dc electric fields [1]. However, the most customary use of rf current drive in tokamaks is in conjunction with Ohmically driven currents. Recently, the importance of current profile tayloring for the access to improved confinement regimes has been recognized, both theoretically [2] and experimentally [3]. Active real-time control of the current density profile in tokamaks is more easily obtained when the bulk of the plasma current is provided by the dc electric field induced by the Ohmic transformer, but a significant fraction is driven by rf waves at a given location determined by wave resonance, accessibility, and/or absorption conditions. A substantial contribution to the total current from the bootstrap effect [4] would make such a scheme attractive for reactor applications. The non-inductive current drive effect is due to the asymmetric decrease of the electron collision rate caused by resonant absorption of rf power. The same decrease also implies an enhancement of the electrical conductivity [5]. This effect is related to the creation of a superthermal electron tail, and must not be confused with the well-known enhancement of the Spitzer conductivity [6] $\sigma_{sp} \propto T_e^{3/2}$, resulting from any electron heating process (where T_e is the electron temperature). That the driven current is larger than the sum of an inductively driven part, evaluated from σ_{sp}, and a purely non-inductive one, evaluated from the Fisch-Boozer formula [7], is a routine experimental observation [e.g., 8-11]. What is more difficult [12] is to separate the different components of the driven current, in order to investigate the properties of the rf-enhanced (also called hot) electrical conductivity. In this paper, a method is proposed to determine the purely non-inductive current drive efficiency η_0 and the hot conductivity σ_{hot} simultaneously, based on an rf power scan. The method is described in Sec. 2. An application to Lower-Hybrid (LH) current drive experiments in the PBX-M tokamak [13] is also performed, as a proof of principle, and presented in Sec. 3. It is also shown that knowledge of both η_0 and σ_{hot} may help in determine quantities such as the

average absorbed wave power fraction and parallel refractive index, which adds valuable information on the process of LH wave absorption. The conclusions are drawn in Sec. 4.

2. Description of the method

Following Ref. [5], the plasma current I_p in the presence of both an inductive loop voltage V and an externally injected rf power P_{in} is written as

$$I_p = I_{ohm} + I_{rf} + I_{hot} + \ldots \quad (1)$$

where $I_{ohm} = V/R_{sp}$ is the purely Ohmic part, R_{sp} is the Spitzer resistance (or, more generally, the neo-classical one), $I_{rf} = \eta_0 P_{in}/n_e R_0$ is the purely non-inductive part that would be driven in the same plasma conditions but V = 0, n_e is the electron density, and R_0 is the tokamak major radius. $I_{hot} = V/R_{hot}$ is the first cross term, proportional to both loop voltage and rf power, R_{hot} is the hot resistance, inversely proportional to $\int \sigma_{hot} dS$, i.e., the cross-section integrated σ_{hot}. The neglected terms in Eq. (1) are the higher-order cross-terms, proportional to PV^2, VP^2, P^2V^2, and so on. The general theoretical expression of the hot conductivity is found in Ref. [5]. In the particular case (pertinent to LH current drive) of wave-particle interaction by diffusion in $v_{||}$ (parallel velocity) and a peaked wave spectrum, resonant at a given $v_{||}$ and zero perpendicular velocity, σ_{hot} is given by

$$\sigma_{hot} = \left(\frac{e^2 n_e}{m \nu_e}\right) \frac{2}{3+Z} \left(\frac{v_{||}}{v_{th}}\right)^4 \frac{p_{abs}}{n_e \nu_e T_e} \quad (2)$$

where e and m are the electron charge and mass, respectively, ν_e is the bulk electron collision frequency, Z is the effective ion charge number, $v_{th} = (T_e/m)^{1/2}$, and p_{abs} is the absorbed rf power density.

The different components of the driven current are illustrated in Fig. 1, obtained by means of a 3-D Fokker-Planck code [14], run for typical parameters of the PBX-M tokamak (minor radius a = 0.3 m, R_0 = 1.65, magnetic field B = 1.5 T, LH wave power P = 540 kW, launched parallel refractive index spectrum peaked at $n_{||} \approx 1.5$) and a homogeneous plasma with

$n_e = 2 \times 10^{19}$ m^{-3}, T_e = 1 keV, Z = 3. The total current is made up of a part (I_{rf}) indipendent of V, an Ohmic part (I_{ohm}) linear in V, I_{hot} which is also linear in V, but with a different slope, and an additional part, well fitted by a V^2 curve, corresponding to the neglected terms in Eq. (1), and becoming non-negligible at high values of V. Now, most rf current drive experiments (and in particular on PBX-M) are performed at constant plasma current, and to each mechanism responsible for current generation corresponds a relative drop in the loop voltage. The total loop-voltage drop is defined as

$$-\frac{\Delta V}{V_{ohm}} \equiv \frac{V_{ohm} - V}{V_{ohm}} = \frac{I_p - I_{ohm}}{I_p} \tag{3}$$

where V_{ohm} is the loop voltage in the Ohmic phase. The loop-voltage drop is also computed with the Fokker-Planck code and the same parameters, but a constant current I_p = 250 kA and various power levels. $-\Delta V/V_{ohm}$ is represented in Fig. 2 (squares) as a function of the wave power normalized to $n_e I_p R_0$: this is just the inverse of an efficiency parameter, represented on the upper scale. For simplicity, the electron temperature is assumed constant: this is approximately true if the wave power is comparable to the Ohmic power (as it is the case in the PBX-M experiment). If there were no conductivity enhancement, the non-inductively driven current would replace the Ohmic current, and the loop voltage drop would grow linearly with power from zero to one (dashed line). The hot conductivity is responsible for the curvature of $-\Delta V/V_{ohm}$ vs P, owing to the fact that the current drive process is more and more efficient for increasing loop voltage. The contribution of the hot conductivity to the loop voltage drop vanishes for $P \rightarrow 0$ and for $V \rightarrow 0$ (i.e. for $-\Delta V/V_{ohm} \rightarrow 1$) and is maximum in between (thick solid curve). It is possible to separate the two contributions when the slope of the dashed line (i.e. the equivalent current drive efficiency for V = 0) is known, but this requires the knowledge of the wave power for which $-\Delta V/V_{ohm} = 1$, namely to realize a full non-inductive current drive experiment for the same plasma parameters, which is often impossible and always difficult.

A simple, though approximate, solution to this problem is the following. Combining Eqs. (1) and (3), as well as the definitions of the various current components, yields

$$-\frac{\Delta V}{V_{ohm}} = 1 - \frac{1 - \eta_0 \dfrac{P_{in}}{n_e I_p R_0}}{1 + \dfrac{R_{sp}}{R_{hot}}} \tag{4}$$

Upon defining: $x = P_{in}/n_e I_p R_0$, and $\eta_1 = R_{sp}/(xR_{hot})$, Eq. (4) becomes

$$-\frac{\Delta V}{V_{ohm}} = \frac{(\eta_0 + \eta_1)x}{1 + \eta_1 x} \tag{5}$$

Note that, since σ_{hot} is proportional to P_{in}, η_1 is independent of power. If data at several power levels and similar global plasma parameters are available, Eq. (5) can be used to determine η_0 and η_1 simultaneously, by means of a simple two-parameter least-squares fit, even if data at $-\Delta V/V_{ohm} = 1$ are missing. A first example of the accuracy of such a procedure is given by the curve connecting the squares on Fig. 2, which has been computed in this way. The values obtained for η_0 and η_1 (in units of $10^{19} AW^{-1}m^{-2}$) are: $\eta_0 = 1.552 \pm 0.008$, $\eta_1 = 0.889 \pm 0.026$, with a linear correlation coefficient of the fit $R = 0.99994$ ($R = 1$ corresponding to a perfect fit). Note that the value found for η_0 corresponds precisely (within an error of 0.3%) to the inverse abscissa $\eta = 1/x$ of the point $-\Delta V/V_{ohm} = 1$, i.e., the current drive efficiency for $V = 0$. Such a good agreement also proves that, in this range of parameters, higher order cross terms are negligible.

Equation (5) is an approximation, in two respects mainly: i) in its derivation it is assumed that the Spitzer resistance in the rf phase is the same as in the Ohmic phase, which is not generally true; ii) quadratic terms have been neglected in Eq. (1), the most important one being the PV^2 term. These limitations are easily removed, although the price to be paid is that Eq. (5) becomes more complex. For instance, if ρ is the ratio of the Spitzer conductivities in the rf and in the Ohmic phase (generally, $\rho \geq 1$), Eq. (5) becomes

$$-\frac{\Delta V}{V_{ohm}} = \frac{(\rho - 1) + (\eta_0 + \rho\eta_1)x}{\rho(1 + \eta_1 x)} \tag{6}$$

Alternatively, Eq. (5) can still be used, but replacing ΔV with a new quantity ΔV^*, defined as

$$-\frac{\Delta V^*}{V_{ohm}} = \rho\left[\left(-\frac{\Delta V}{V_{ohm}}\right) - \left(-\frac{\Delta V}{V_{ohm}}\right)_{P\to 0}\right] = \rho\left[\left(-\frac{\Delta V}{V_{ohm}}\right) - \left(1 - \frac{1}{\rho}\right)\right] \tag{7}$$

where the second term in the brackets denotes the limit for vanishing rf power. The presence of a fraction of bootstrap current $\phi = I_{bs}/I_p$ (ϕ_{ohm} in the Ohmic phase) can also be included in Eq. (6), which becomes

$$-\frac{\Delta V}{V_{ohm}} = \frac{\left(\rho - \frac{1-\phi}{1-\phi_{ohm}}\right) + \left(\frac{\eta_0}{1-\phi_{ohm}} + \rho\eta_1\right)x}{\rho\left(1+\eta_1 x\right)} \tag{8}$$

The presence of an additional term in Eq. (1), e.g., a current I_q proportional to P and quadratic in V, i.e. $I_q = V/R_q$, where the resistance R_q is proportional to 1/(PV), yields the following generalization of Eq. (5):

$$-\frac{\Delta V}{V_{ohm}} = 1 - \frac{1+\eta_1 x}{\eta_2 x}\left\{\left[1 + 2\eta_2 x \frac{1-\eta_0 x}{\left(1+\eta_1 x\right)^2}\right]^{1/2} - 1\right\} \tag{9}$$

where $\eta_2 = (2I_p R_{sp}^2)/(R_q V x)$ is independent of P and V. In the limit $\eta_2 \to 0$, Eq. (9) reduces to Eq. (5). The use of Eq. (9) is, of course, limited to the analysis of very good data, since it implies a three-parameter fit. Finally, note that the actual current drive efficiency in the presence of a non-zero loop voltage is generally given by $\eta = (-\Delta V/V_{ohm})/x$. Its expression as a function of $\eta_{0,1,2}$ can be immediately deduced, at the different levels of approximation considered, from Eqs. (5), (6), (8), and (9).

Before using the above described method to analyze experimental data, some comments are needed. The method is general, in the sense that no assumption has been made concerning the dependences of η_0 and η_1 on the various plasma and wave parameters. However, using the well known theoretical expressions for the current drive efficiency [7], hot [5], and Spitzer [6] conductivities, it is found that

$$\eta_0 \propto \frac{1}{5+Z}\frac{1}{n_{\|abs}^2} \quad , \quad \eta_1 \propto \frac{Z}{3+Z}\frac{1}{n_{\|abs}^4}\frac{I_p}{n_e T_e^{3/2}}$$

where $n_{\|abs}$ is an average parallel refractive index at the location where the waves are effectively absorbed, generally depending on several plasma parameters. These relations show that the fitting technique we propose should be applied to a rather homogeneous data set. Fortunately, the dependence in Z of both η_0 and η_1 are rather weak; the parametric dependence of η_1

suggests that keeping the parameter $I_p/(n_e T_e^{3/2})$ fixed is beneficial for the accuracy of the determination of η_1. The most critical problem is the temperature dependence of $n_{\|abs}$, which is the result of very complicated physics processes and is not always easy to predict [13]. Conditions in which the LH power input is comparable to the Ohmic input are particularly suited to the application of the method in its simplest form, since the LH power progressively replaces the Ohmic power, and the temperature variations are small. This is the case for the PBX-M data discussed in the next section.

3. Experimental results

We now apply Eq. (5) to experimental data, measured during LH current drive experiments on the PBX-M tokamak [13]. The experiments were performed either in circular or in indented (bean-shaped) plasma configurations. Typical parameters were: $I_p \approx 100$ - 200 kA, $n_{e0} \approx 1$ - 3×10^{19} m^{-3}, $B \approx 1.4$ - 1.7 T, $Z \approx 3$, $T_{e0} \approx 0.6$ - 1.4 keV, $V = 0.3$ -1.3 Volts. Wave power up to 500 kW, at 4.6 GHz, was delivered to the plasma through two fully-phased arrays of 32 waveguides each [15]. Data were taken injecting 5 values of parallel refractive index $n_{\|in}$, with the peaks between 1.45 and 2.75. The coupled wave power was, at best, sufficient to induce a loop voltage drop of 80%. In Ref. [13], the data have been analyzed using the so-called Karney-Fisch method [16,17], originally developed to analize current ramp-up experiments and subsequently extended to steady-state regimes [10]. Basically, this consists in plotting the quantity P_{el}/P_{abs} (where P_{abs} is the total absorbed wave power and $P_{el} = VI_p(-\Delta V/V_{ohm})$) versus $u = v_{ph}/v_D$, where v_{ph} is the dominant wave phase velocity of the wave-particle interaction and v_D is the Dreicer velocity. Now, $v_{ph} = c/n_{\|abs}$, where c is the speed of light and $n_{\|abs}$ is related to the injected index $n_{\|in}$ through an unknown upshift factor $\beta = n_{\|abs}/n_{\|in}$. The absorbed wave power as well is related to the injected wave power through a constant of proportionality $\alpha = P_{abs}/P_{in}$. Comparison of the experimental curve with a theoretical expression [17] containing as basic ingredients the factors α and β allows the

determination of the equivalent current drive efficiency η_0 and of $n_{||abs}$. However, in this method, the combination of values of α and β reproducing the experimental results is not unique, and additional assumptions are required: for instance, in Refs. [10,13,16] a single constant value of $\alpha \approx 0.65$ has been, somewhat arbitrarily, used.

We now analyze the data in a different way: for each injected wave phasing, we plot $-\Delta V/V_{ohm}$ versus x and use a least-squares fit to determine η_0 and η_1. The theory in its simple form (Eq. (5)) is used, after correction of the data for modest changes in the Spitzer conductivity between the Ohmic and the rf phases, which is equivalent to using Eq. (7). Moreover, the bootstrap current is negligible in this regime, and neoclassical corrections to the Spitzer conductivity have also been neglected, on the basis of previous studies of the PBX data [18]. The data and the fits for both circular and bean-shaped plasmas and $n_{||in} = 2.08$ are shown in Fig. 3. The variations of x are mainly associated with a power scan (50 - 500 kW). The magnetic field was constant (1.4 T and 1.7 T for circular and bean-shaped plasmas, respectively) The standard deviations of the other plasma parameters over the data set are the following: $\Delta n_e \sim 35$ %, $\Delta I_p \sim 20$ %, $\Delta T_e \sim 12$ % and 15 % (for circular and bean-shaped plasmas, respectively), $\Delta[I_p/(n_e T_e^{3/2})] \sim 35$ %. This qualifies the data set as moderately suited for this type of analysis, thus representing a good test. The main difference between the circular and bean-shaped plasmas is the temperature, which is 50 to 100 % higher in the bean-shaped configuration; this implies differences in $n_{||abs}$ as well. The best-fit parameters are: $\eta_0 = 0.33 \pm 0.03$, $\eta_1 = 0.36 \pm 0.07$, $R = 0.97$ (circular); $\eta_0 = 0.72 \pm 0.11$, $\eta_1 = 0.74 \pm 0.23$, $R = 0.96$ (bean). This is a satisfactory fit, taking into account the fact that data at (moderately) different densities, currents and temperatures were used. Moreover, the values of η_0 are in close agreement with those obtained in Ref. [13] by means of the Karney-Fisch method (0.37 and 0.64, respectively). Once η_0 and η_1 are known, the different components of the plasma current can be separated. An example is shown in Fig. 4, where the inductive part of the plasma current $I_p - I_{rf} = I_{ohm} + I_{hot}$ is shown versus the applied loop voltage, for a circular plasma and two sets of experimental points, taken from those of Fig. 3 (at nearly constant n_e). Both sets

are characterized by the same total plasma current ($I_p \approx 120$ kA), but two different values of the injected wave power and therefore also of the plasma temperature ($P_{in} \approx 300$ kW, $T_{e0} \approx 0.8$ keV for the group of points at low V; $P_{in} \approx 150$ kW, $T_{e0} \approx 0.65$ keV for the group of points at high V). Comparison with the purely Ohmic current I_{ohm} (open circles) shows that the change in the slopes of the linear fits (straight lines) due to the decreased plasma resistance is large for high wave power, and that the hot conductivity effect can be responsible for a significant fraction of the total plasma current.

The analysis has then been applied to different wave phasings in circular and bean-shaped configurations: this way we could evaluate η_0 and η_1 for 8 different values of $n_{\|abs}$, and compare their $n_\|$ dependencies to those expected from theory [5,7], i.e., $\eta_0 \propto n_\|^{-2}$ and $\eta_1 \propto n_\|^{-4}$. η_0 and η_1, determined by means of the new method, are plotted versus $n_{\|abs}$, obtained from the Karney-Fisch method with constant $\alpha = 0.65$, in Figs. 5 (a) and (b), respectively, and are compared with a general power-law fit of the type $y = px^q$. The expected $n_\|$ dependencies are accurately reproduced, and the constants in front of the power-law are in fairly good agreement with the theoretical ones, evaluated for average values of density and temperature.

Since the method proves satisfactory, it is attractive to fully exploit its potential. Note that $\eta_0 \propto \alpha/\beta^2$, and $\eta_1 \propto \alpha/\beta^4$ (see Eq. (2)), where $\alpha = P_{abs}/P_{in}$ and $\beta = n_{\|abs}/n_{\|in}$. Thus

$$\beta \propto \sqrt{\frac{\eta_0}{\eta_1}} \quad , \qquad \alpha \propto \frac{\eta_0^2}{\eta_1} \tag{10}$$

the constants of proportionality being those of [5,7], i.e.,

$$\frac{\beta}{\sqrt{\eta_0/\eta_1}} = \left(\frac{c}{n_{\|in} v_{th}}\right)\left[\frac{5+Z}{2(3+Z)}\frac{I_p}{n_e|e|v_{th}}\frac{\left(e^2 n_e/m\nu_e\right)}{\int \sigma_{sp} dS}\right]^{1/2}$$

$$\frac{\alpha}{\eta_0^2/\eta_1} = \frac{\pi}{4}\frac{(5+Z)^2}{3+Z}\frac{I_p}{n_e|e|v_{th}}\frac{\left(e^2 n_e/m\nu_e\right)}{\int \sigma_{sp} dS}\frac{T_e \nu_e}{n_e|e|v_{th}} \tag{11}$$

where $\int\sigma_{sp}dS$ is the cross-section integrated Spitzer conductivity. Note that the use of Eqs. (10,11) is subject to the same restrictions as that of the general method (i.e., modest variations of the parameter $I_p/(n_e T_e^{3/2})$), and that, over each of the data sets considered, the temperature variations were not larger than 15 %. From Eq. (10), both α and β are determined, without

any additional assumption, if the quantities appearing in Eqs. (11) are also measured. An example of this procedure is given by Figs. 6 and 7. In Fig. 6, $n_{\|abs}$, obtained from Eq. (10), is plotted versus $n_{\|in}$ (open squares). As extensively discussed in Ref. [13], for $n_{\|in} < 2$ the plasma core is not accessible to the waves, and the rays need a larger upshift to be absorbed. The $n_{\|abs}$ evaluated from the Karney-Fisch method with the assumption $\alpha = 0.65$ (full squares), substantially displays the same behaviour, with some small quantitative differences. The advantage of the new method is that now the fraction of absorbed power is also determined for every injected phase, as shown in Fig. 7, where α is plotted versus $n_{\|abs}$, both determined from η_0 and η_1. It appears that the average value of α is not far from 0.65, but α is definitely not constant, and it exhibits a nearly linear dependence on $n_{\|abs}$. This trend is reasonable, since higher-$n_{\|}$ waves resonate more in the bulk of the electron distribution and therefore are more absorbed. Conversely, that the complex physics involved in the ray propagation process, and yielding large $n_{\|}$ upshifts, results into such a simple linear dependence should first be confirmed on a wider data base and then be the subject of a more detailed analysis.

An additional point that can be elucidated in a simple way is the effect of the antenna directivity. It is well known that generally the launched spectra have at least a secondary lobe, usually at values of $n_{\|}$ that are higher in absolute value and opposite in sign. The ratio $\rho_{\pm}$ of the power launched in the main lobe to that in the secondary lobe is generally dependent on the wave phasing, which could, in principle, change the results of Fig. 7. Introducing two fractions of absorbed power for the main and the secondary lobe, α_+ and α_-, respectively, and two absorbed parallel refractive indices n_+ and n_-, and using the theoretical expressions for current drive efficiency [7] and σ_{hot} [5], it is found that

$$\eta_0 \propto \frac{1}{1+\rho_{\pm}}\left(\frac{\alpha_+}{n_+^2} - \rho_{\pm}\frac{\alpha_-}{n_-^2}\right) \quad , \qquad \eta_1 \propto \frac{1}{1+\rho_{\pm}}\left(\frac{\alpha_+}{n_+^4} + \rho_{\pm}\frac{\alpha_-}{n_-^4}\right) . \tag{12}$$

Note that the contributions of the two lobes to the non-inductive current subtract, whereas those to the hot conductivity add. Since, generally, the injected $n_{\|}$ of the secondary lobe is significantly larger than that of the main lobe, a good assumption is that the secondary lobe is

fully absorbed without any significant upshift, thus n_- is the same as the injected value, and $\alpha_- \approx 1$. With these assumptions, it is possible to evaluate α_+ and n_+ from Eqs. (12). The result is still a linear dependence of α_+ from n_+, with a slight upwards displacement of the straight line $\alpha_+(n_+)$. In conclusion, the linear behaviour of Fig. 7 is not substantially affected by antenna directivity effects.

4. Conclusions

A relatively simple method has been developed for the analysis of rf current drive experiments in the presence of a residual loop voltage. In these regimes, that are the most currently studied in experiments, it is difficult to isolate the two most important transport coefficients: the equivalent current drive efficiency at $V = 0$, and the hot electrical conductivity. The analysis proposed here applies to regimes in which the bilinear (in wave power and electric field) cross term is the dominant one, which excludes cases of abundant runaway generation. In this limit, an explicit relation between the loop voltage drop and the injected wave power has been established. The new method consists in using this relation to determine space-averaged values of the two relevant transport coefficients from global measurements of the loop-voltage drop at various power levels. The method is not related to a particular theory, but only to definitions of basic quantities, and its application consists in a straightforward two-parameter fit. Of course, it has the basic limits of every zero-dimensional approach. A proof of principle has been given, applying the method to LH current drive experiments in PBX-M. This has revealed the potential of this analysis technique to provide a valuable insight into the specific problem of LH wave propagation and absorption. The main result of this analysis of the PBX-M experiments is that the fraction of absorbed power is found to be a linear function of the absorbed $n_{||}$. Note that α and β are both determined from the current drive efficiency and the hot conductivity, thus they have to be interpreted as average or representative values of power absorption and upshift factors, related to the part of the spectrum that effectively drives

currents. In this approach, the power directly absorbed by the bulk of the electron distribution or through collisional processes at the plasma edge is considered as lost. Conversely, the analysis can be easily extended to include wave spectra having lobes at both positive and negative $n_{\|}$.

Acknowledgements

This work was partially supported by USDOE under Contract AC02-76-CH0-3073.

References

[1] Fisch N.J., Rev. Mod. Phys. **59** (1987) 175.

[2] Ozeki T., Azumi M., Tokuda S., Ishida S., Nucl. Fusion **33** (1993) 1025; Kessel C., Manickam J., Rewoldt G., Tang W.M., Phys. Rev. Lett. **72** (1994) 1212; Turnbull A.D., Taylor T.S., Lin-Liu Y.R., St. John H., Phys. Rev. Lett. **74** (1995) 718.

[3] Lazarus E.A., et al., Phys. Fluids **B4** (1992) 3644; Goldston R.J., Plasma Phys. Contr. Fusion **36** (1994) B213; Litaudon X., et al., Plasma Phys. Contr. Fusion **38** (1996) 1603.

[4] Bickerton R.J., Connor J.W., Taylor J.B., Nature **229** (1971) 110.

[5] Fisch N.J., Phys. Fluids **28** (1985) 245.

[6] Spitzer L., Härm R., Phys. Rev. **89** (1953) 977.

[7] Fisch N.J., Boozer A.H., Phys. Rev. Lett. **45** (1980) 720.

[8] Leuterer F., Söldner F., Eckhartt D., et al., Plasma Phys. Contr. Fusion **27** (1985) 1399; Yoshioka K., Okazaki T., Leuterer F., Fujisawa N., Phys. Fluids **31** (1988) 1224.

[9] Takase Y., Knowlton S., Porkolab M., Phys. Fluids **30** (1987) 1169.

[10] Bizarro J.P., Hoang G.T., Berger-By G., et al., in *Controlled Fusion and Plasma Physics* (EPS, Geneva, 1991), **15C** III, 357; D. Moreau and the Tore Supra Team, Phys. Fluids **B4** (1992) 2165.

[11] James R.A., Giruzzi G., De Gentile B., et al., Phys. Rev. A **45** (1992) 8783.

[12] Forest C.B., Kupfer K., Luce T.C., Politzer P.A., Lao L.L., Wade M.R., Whyte D.G., Wròblewski D., Phys. Rev. Lett. **73** (1994) 2444.

[13] Bernabei S., Cardinali A., Giruzzi G., Hoang G.T., Ignat D., Kaita R., Okabayashi M., Paoletti F., Von Goeler S., Phys. Plasmas **4** (1997) 125.

[14] Giruzzi G., Plasma Phys. Contr. Fusion **A35** (1993) 123.

[15] N. Greenough, S. Bernabei, M. Norris, S. Schweitzer, R. Schwartz, 14th IEEE Symp. on Fus. Eng. S. Diego (Oct 1991) vol. 1, p. 126.

[16] Karney C.F.F., Fisch N.J., Jobes F.C., Phys. Rev. A **32** (1985) 2554.

[17] Karney C.F.F., Fisch N.J., Phys. Fluids **29** (1986) 180.

[18] Kaye S.M., Levinton F.M., Hatcher R., et al., Phys. Fluids **B4** (1992) 651.

Figure Captions

Fig. 1 Computed current vs loop voltage at fixed rf absorbed power P = 540 kW. The squares representing the total driven current I_{tot} are connected by a parabolic fit. The different current components are shown.

Fig. 2 Computed loop voltage drop vs $x = P/n_e I_p R_0$ (lower scale) and vs $\eta = n_e I_p R_0/P$ (upper scale), at fixed plasma current I_p = 250 kA. The curve connecting the squares is a fit of the type $(\eta_0+\eta_1)x/(1+\eta_1 x)$.

Fig. 3 Measured loop voltage drop vs $x = P_{in}/n_e I_p R_0$ (lower scale) and vs $\eta = n_e I_p R_0/P_{in}$ (upper scale), for circular and bean-shaped plasmas, and $n_{\|in} = 2.08$. The curves connecting the circles are fits of the type $(\eta_0+\eta_1)x/(1+\eta_1 x)$. The best fit parameters are: $\eta_0 = 0.33 \pm 0.03$, $\eta_1 = 0.36 \pm 0.07$, R = 0.97 (circular); $\eta_0 = 0.72 \pm 0.11$, $\eta_1 = 0.74 \pm 0.23$, R = 0.96 (bean).

Fig. 4 Inductive part of the plasma current $I_p - I_{rf}$ versus loop voltage, for the shots of Fig. 3 (circular plasma). The set of points at low V corresponds to $P_{in} \approx 300$ kW, $T_{e0} \approx 0.8$ keV; those at high V correspond to $P_{in} \approx 150$ kW, $T_{e0} \approx 0.65$ keV.

Fig. 5 η_0 vs $n_{\|abs}$ (a), and η_1 vs $n_{\|abs}$ (b), obtained by least squares fits of the type shown in Fig. 3, for several values of the launched LH wave phase. $n_{\|abs}$ is evaluated by the Karney-Fisch method. The curves connecting the circles are general power-law fits of the type $y = px^q$. The p and q values obtained are displayed, as well as the linear correlation coefficients of the fit R (R = 1 corresponds to a perfect fit).

Fig. 6 Average absorbed vs injected $n_{\|}$, computed by the new method and by the Karney-Fisch method (with $\alpha = 0.65$), for a circular plasma.

Fig. 7 $\alpha = P_{abs}/P_{in}$ vs $n_{\|abs}$, both determined from η_0 and η_1.

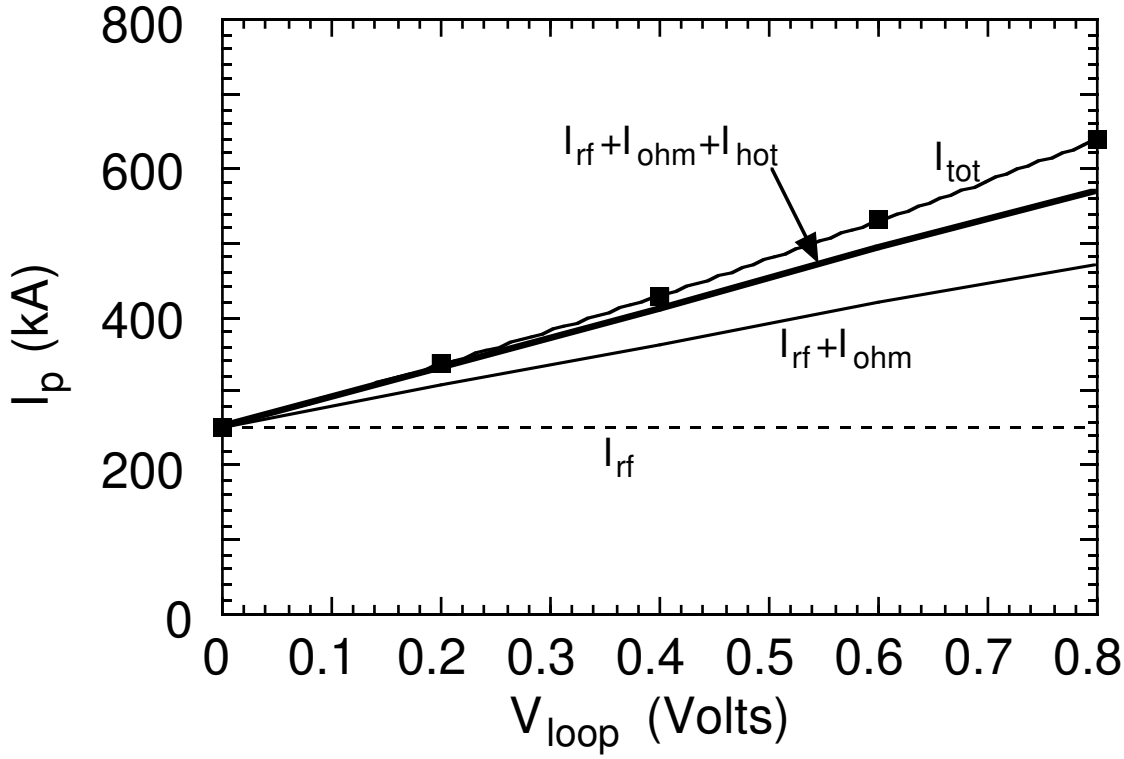
800
600
400
200
0
I_p (kA)
0
0.1
0.2
0.3
0.4
0.5
0.6
0.7
0.8
V_{loop} (Volts)
$I_{rf}+I_{ohm}+I_{hot}$
I_{tot}
$I_{rf}+I_{ohm}$
I_{rf}

Fig. 1

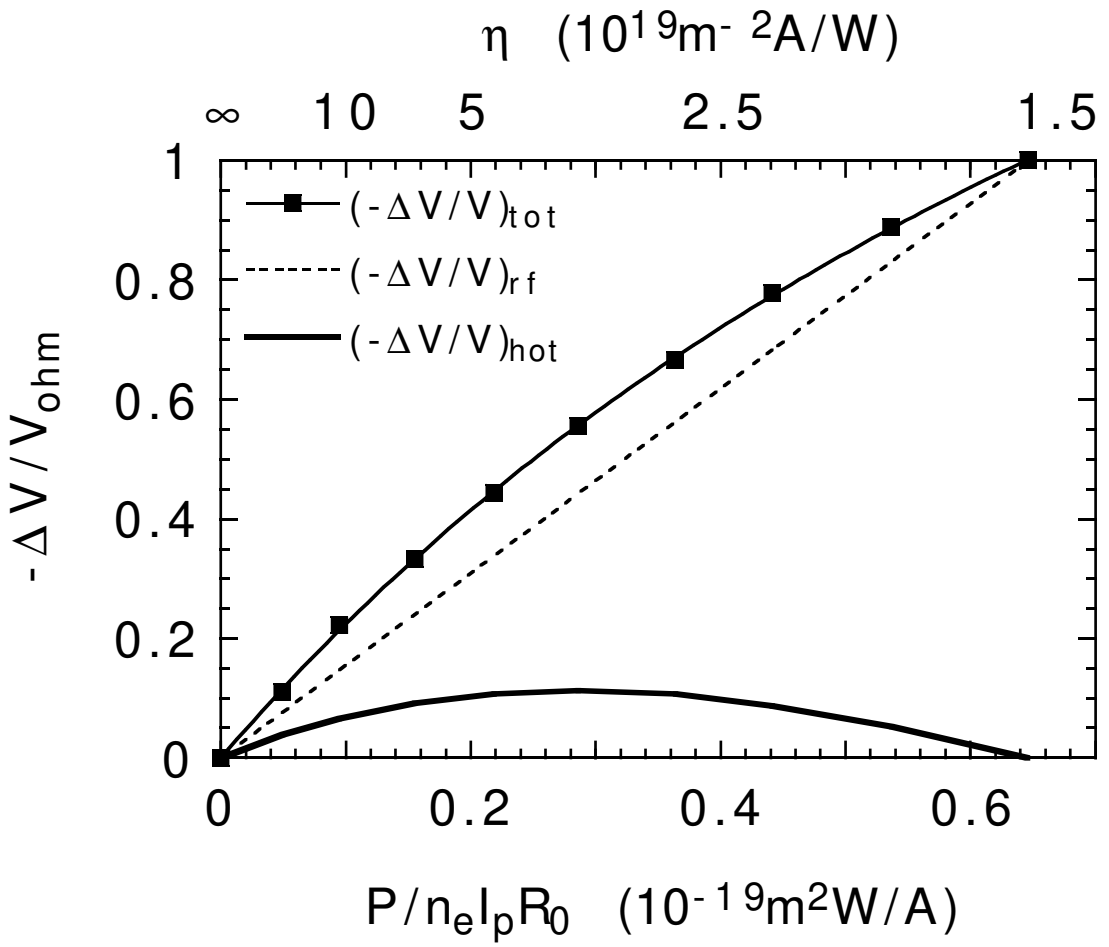
η (10^19 m^-2 A/W)
∞
10
5
2.5
1.5
1
0.8
0.6
0.4
0.2
0
-ΔV/V_ohm
(-ΔV/V)_tot
(-ΔV/V)_rf
(-ΔV/V)_hot
0
0.2
0.4
0.6
P/n_e I_p R_0 (10^-19 m^2 W/A)

Fig. 2

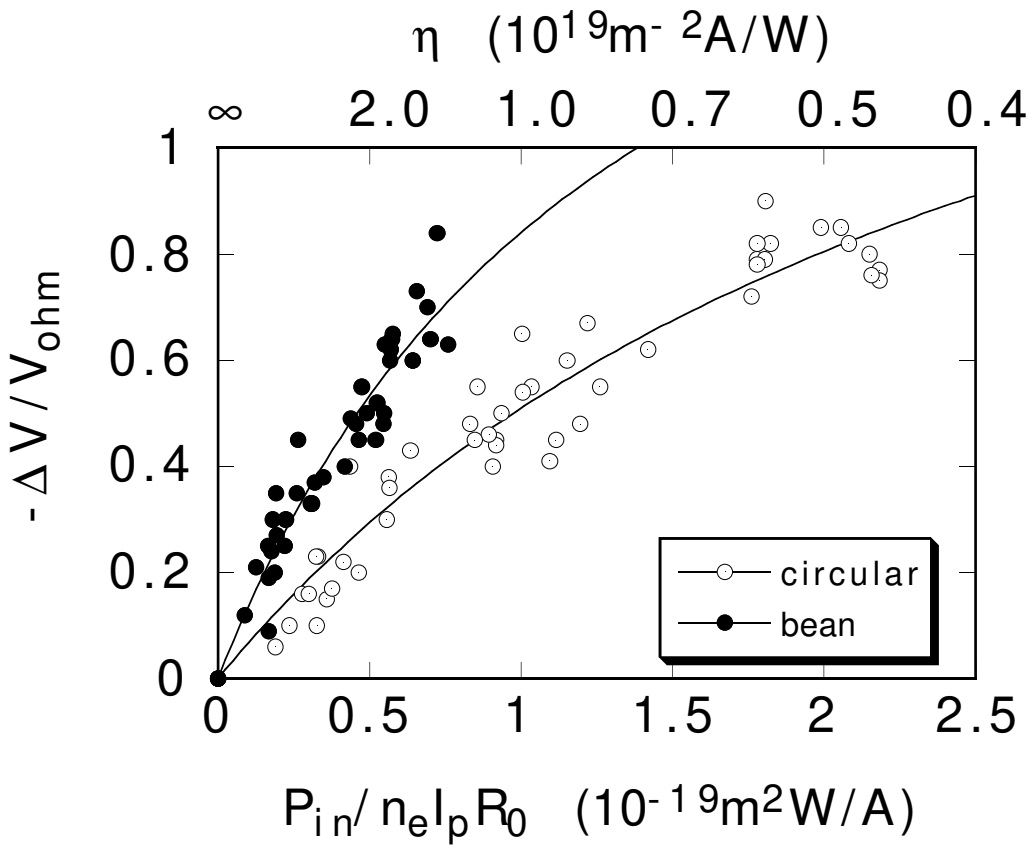
η (10^19 m^-2 A/W)
∞
2.0
1.0
0.7
0.5
0.4
1
0.8
0.6
0.4
0.2
0
-ΔV/V_ohm
0
0.5
1
1.5
2
2.5
circular
bean
P_in/n_e I_p R_0 (10^-19 m^2 W/A)

Fig. 3

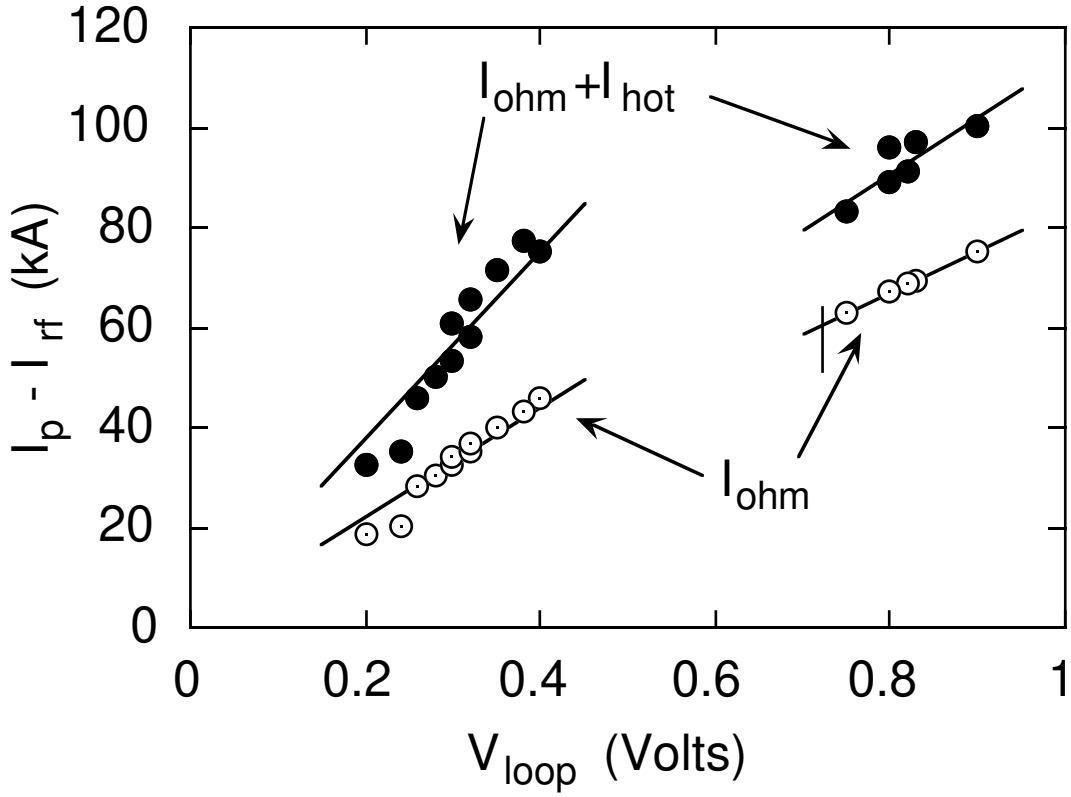
120
100
80
60
40
20
0
0
0.2
0.4
0.6
0.8
1
$I_p - I_{rf}$ (kA)
V_{loop} (Volts)
$I_{ohm} + I_{hot}$
I_{ohm}

Fig. 4

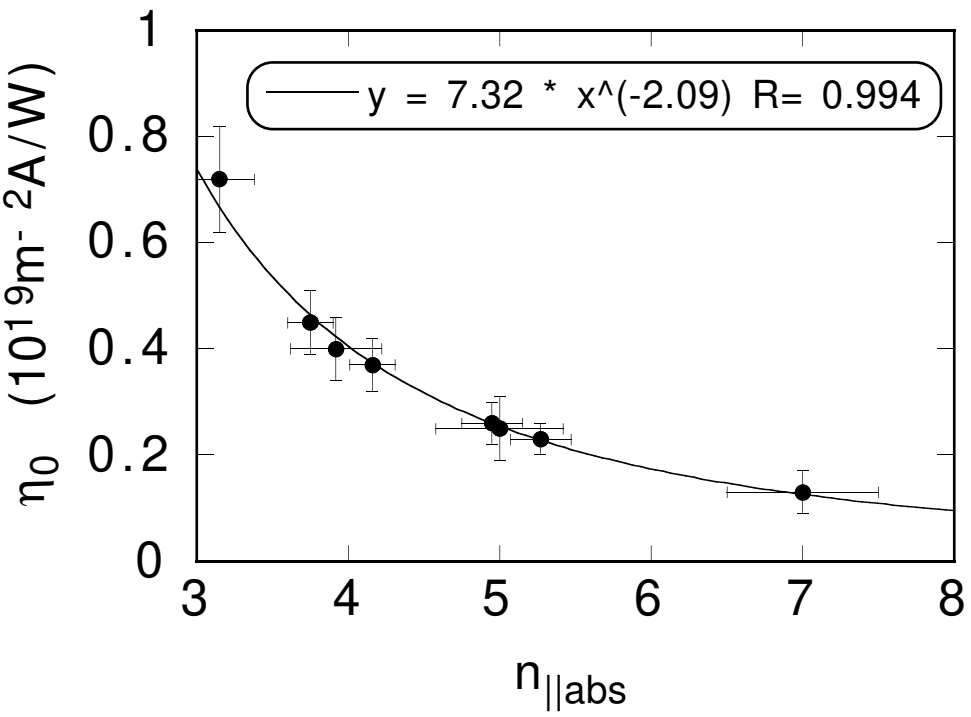

Fig. 5(a)

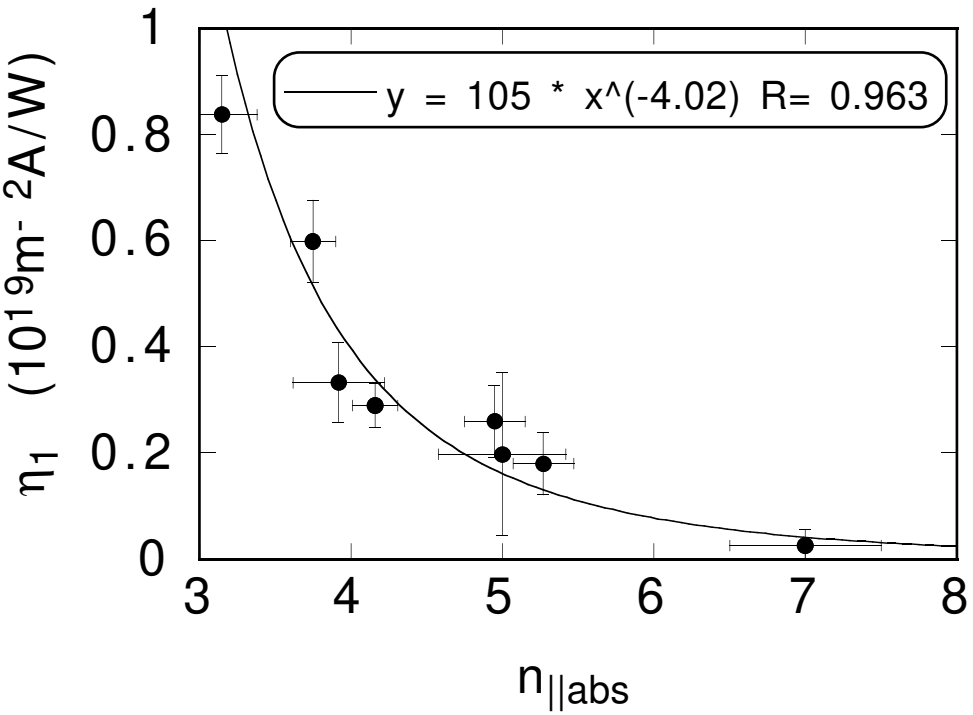

Fig. 5(b)

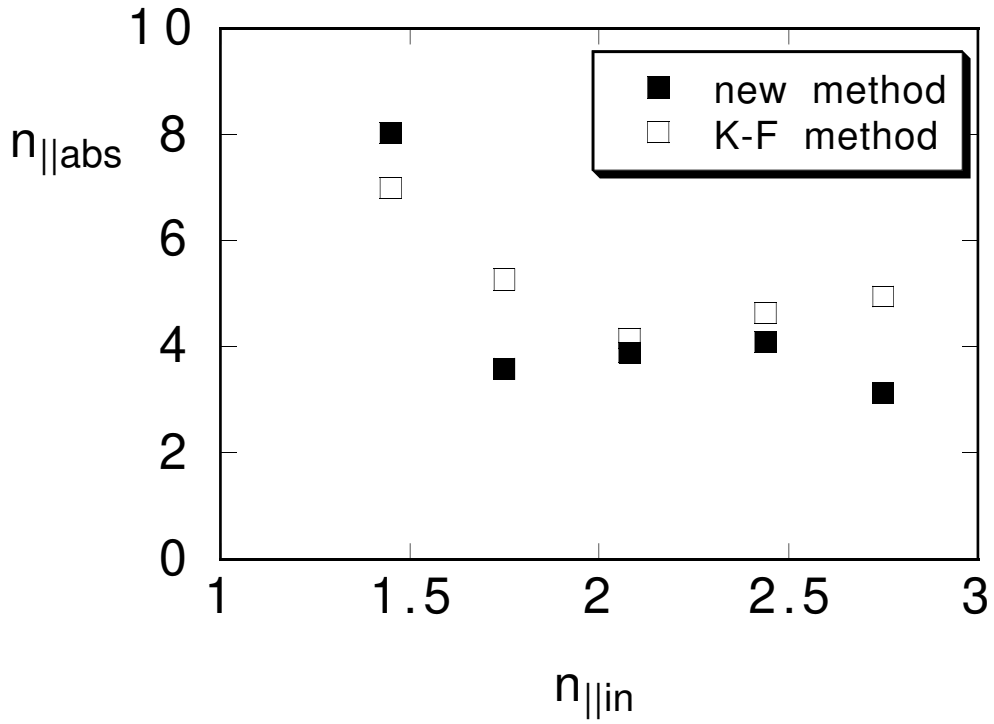

Fig. 6

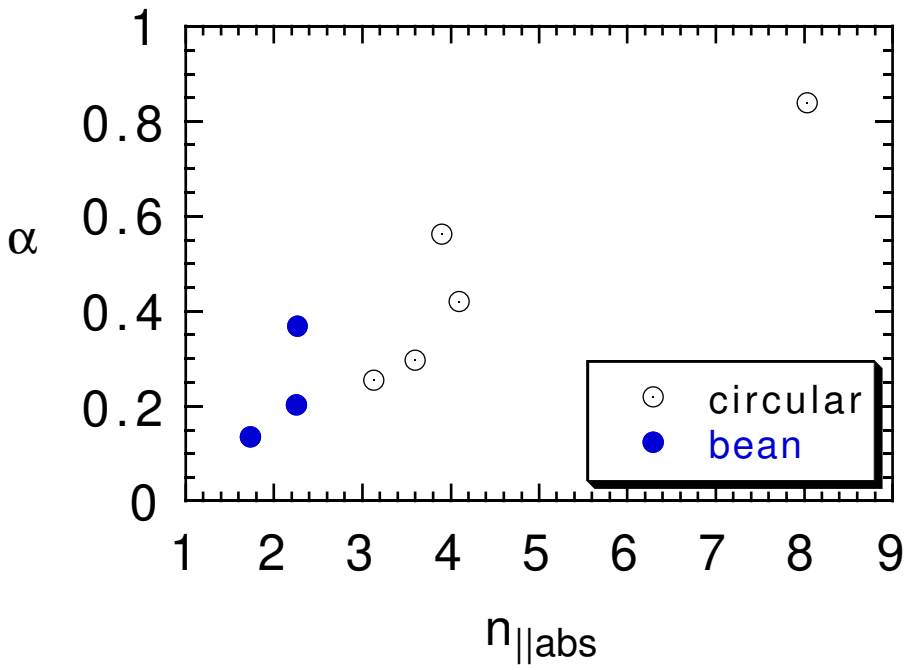

Fig. 7